Geochemical Perspectives Letters

Geochemistry and metallogeny of Neoproterozoic pyrite in oxic and anoxic sediments

J. Parnell[1]*, M. Perez[2], J. Armstrong[1], L. Bullock[1], J. Feldmann[2], A.J. Boyce[3]

OPEN ACCESS

doi: 10.7185/geochemlet.1812

Abstract

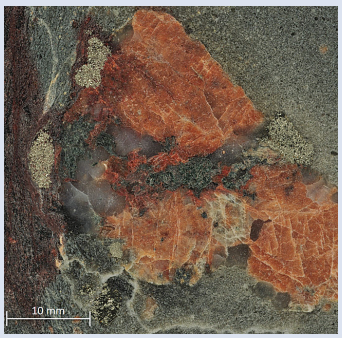

The Neoproterozoic Dalradian Supergroup contains widespread diagenetic sulphides present as pyrite. The sulphides occur in both carbonaceous shales and glacial diamictites, that were deposited in relatively reducing and oxidising conditions respectively. The trace element compositions of the pyrite, and consequently the whole rock compositions, contrast between the two lithologies. The highest concentrations of selenium, tellurium and gold are all found in diamictite-hosted pyrite. The data suggest that increased mobility of these elements in oxidising conditions led to greater uptake when pyrite was precipitated. As one model for the formation of orogenic gold ore deposits assumes a sulphide-rich protolith, pyrite ultimately formed during relatively oxidising conditions could make a contribution, including the widespread pyrite precipitated during the Neoproterozoic 'Snowball Earth' glaciations.

Received 22 November 2017 | Accepted 25 March 2018 | Published 2 May 2018

Introduction

The genesis of some ore deposits, including orogenic gold deposits, is believed to start with the sequestration of metals in diagenetic pyrite that grows in anoxic carbonaceous sediments (*e.g.,* Pitcairn, 2011; Gaboury, 2013; Tomkins, 2013). Pyrite is a product of microbial sulphate reduction at low temperature. Trace elements then become concentrated into vein minerals from this protolith during subsequent metamorphism and deformation. Widespread anoxic black shale deposition in the Neoproterozoic has been linked to a peak in orogenic gold deposits (Tomkins, 2013). Diagenetic pyrite is most widely found in sediment deposited in reducing environments, such as the Neoproterozoic carbonaceous shales. However, the Neoproterozoic diamictites (tillites) deposited during the global glacial events known as 'Snowball Earth' also contain diagenetic pyrite (Parnell and Boyce, 2017). The diamictites represent a more oxidising environment than the carbonaceous shales, and hence a different capacity to incorporate trace elements including economically important metals, which is Eh-controlled. The Neoproterozoic Argyll Group, Dalradian Supergroup (Fig. 1), includes both pyritic carbonaceous shales (Easdale Slate and correlatives) and diamictites (Port Askaig Formation) in Scotland and Ireland. Pyrite occurs disseminated through the shales, and in the diamictite is especially distributed at the surfaces of granite pebbles (Parnell and Boyce, 2017). The Argyll Group thus offers the potential to compare trace element enrichment in both relatively reducing and oxidising environments. This can be measured using a combination of whole rock compositions and the detailed chemistry of diagenetic pyrite. The lithology can be excluded as a contributory factor, as both shale and diamictite have a homogenised provenance. Our results highlight the significance for metallogeny in the Dalradian Supergroup, which includes active gold mines (Fig. 1).

The occurrence of five elements (Se, As, Te, Pb, Au) in pyrite is especially informative. Selenium is the most reliable indicator of seawater chemistry in pyrite samples (Large *et al.,* 2014). Arsenic is commonly the most abundant trace element in pyrite, but varies with degree of oxidation of the depositional environment (Berner *et al.,* 2013). Tellurium was measured, as the Te/Se ratio is also proposed to be influenced by degree of oxidation (Schirmer *et al.,* 2014). Lead tends to be introduced by hydrothermal activity (Tabelin *et al.,* 2012), and thus should be independent of the depositional environment. Gold was measured, as pyrite in carbonaceous shales is considered to be an important source of orogenic gold deposits (Tomkins, 2013).

Methodology

Samples of 35 pyritic shales and 28 diamictites were collected from 21 localities across the entire outcrop length of 450 km in Scotland and Ireland (Fig. 1, Table S-1). This database allowed representative coverage and duplicate sampling. At most localities the sediments are weakly metamorphosed to greenschist facies.

1. School of Geosciences, University of Aberdeen, Aberdeen AB24 3UE, UK
2. Trace Element Speciation Laboratory (TESLA), Department of Chemistry, University of Aberdeen, Aberdeen AB24 3UE, UK
3. Scottish Universities Environmental Research Centre, East Kilbride, Glasgow G75 0QF, UK
* Corresponding author (email: J.Parnell@abdn.ac.uk)

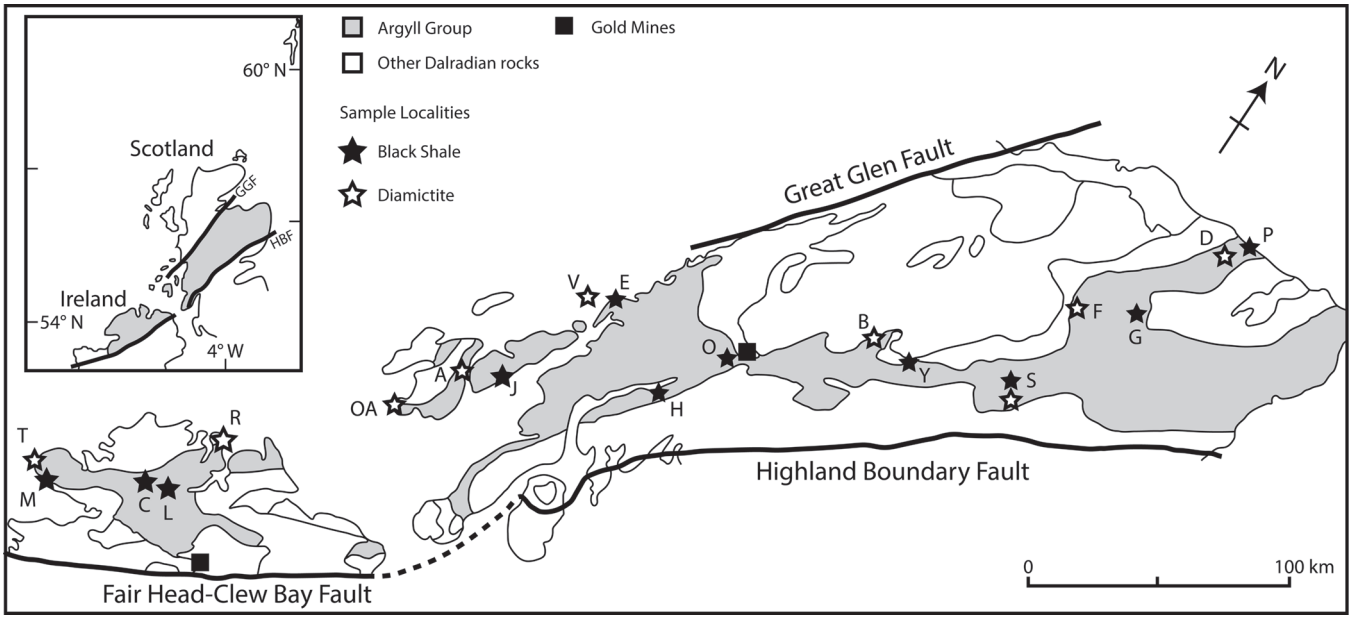

Figure 1 Sample map (after Prave *et al.*, 2009). A, Port Askaig; B, Balmore; C, Cullion; D, Fordyce; E, Easdale; F, Meikle Fergie Burn; G, Glenbuchat; H, Strachur; J, Jura Forest; K, Kerrera; L, Bellanamore; M, Muckross; O, Strath Orchy; OA, Mull of Oa; P, Portsoy; R, Croaghan Hill; S, Glen Shee; T, Kiltyfannad/Glencolumbkille; V, Garvellachs; Y, Aberfeldy-Foss.

Trace element contents were measured in whole rock samples using inductively coupled plasma mass spectrometry (ICP-MS). Samples of ~30 g rock were milled and homogenised, and 0.25 g digested with perchloric, nitric, hydrofluoric and hydrochloric acids to near dryness. The residue was topped up with dilute hydrochloric acid, and analysed using a Varian 725 instrument. Samples with high concentrations were diluted with hydrochloric acid to make a solution of 12.5 mL, homogenised, then analysed by ICP-MS. The limits of detection/resolution are 0.05 and 10,000 ppm.

Trace element analysis of pyrite in 29 shales, and 22 diamictites was performed using a New Wave laser ablation system UP213nm (New Wave Research, Fremont, CA) coupled to a inductive coupled plasma mass spectrometer (ICP-MS) Agilent 7900. The laser beam had a round spot size of 100 μm moving in a straight line, 10 Hz repetition rate and 50 μm s^{-1} ablation speed with 1 J/cm^2 energy. Before ablation, a warm-up of 15 s was applied with 15 s delay between each ablation. The following isotopes were monitored (dwell time): ^{57}Fe (0.001 s), ^{65}Cu (0.001 s) ^{75}As (0.05 s), ^{78}Se (0.1 s), ^{82}Se (0.1 s), ^{107}Ag (0.1 s), ^{125}Te (0.1 s), ^{126}Te (0.1 s), ^{197}Au (0.1 s), ^{208}Pb (0.05 s) and ^{209}Bi (0.1 s). Setting parameters were optimised daily by using NIST Glass 612, to obtain the maximum sensitivity and to ensure low oxide formation. In order to remove possible interferences, a reaction cell was used with hydrogen gas. The MASS-1 Synthetic Polymetal Sulfide standard (USGS, Reston, VA) was used to provide semi-quantification by calculating the ratio of concentration (μg g^{-1})/counts *per* second, and multiplying this ratio by the sample counts. Counts for Se, As, Te, Au and Pb were based on >100 measurements *per* sample, and thereafter converted to concentrations (ppm).

Results

Mean whole rock values for many trace elements in shales (Ag, Bi, Co, Cu, Mo, Pb, Se, Te, Zn) are equal to or higher than global mean values for shales (Supplementary Information), whereas mean values for some trace elements in diamictites are lower than global mean values for shales. However, the mean values for Se, Te, Cu, Co and V are higher in the diamictites than in the shales, for example Se (diamictites 2.6 ± 1.1 ppm, shales 2.1 ± 1.5 ppm, global mean shales 1.3 ppm) and Te (diamictites 0.13 ± 0.05 ppm, shales 0.07 ± 0.07 ppm, global mean shales 0.05 ppm). Au was not measured in whole rock samples.

The relative concentrations of rhenium (Re) and molybdenum (Mo) in the whole rock samples allow assessment of the degree of oxygenation in the depositional environments (Crusius *et al.*, 1996). A Re/Mo ratio of about 0.005 wt./wt. separates samples deposited in suboxic concentrations (higher ratios) from those deposited in anoxic environments (lower ratios). The samples of diamictite have higher Re/Mo ratios (mean ratio value 0.007) than the samples of shale (0.001). Schirmer *et al.* (2014) proposed, from a limited data set, that the Te/Se ratio may also be influenced by degree of oxidation, hence may vary with depositional environment. The mean Te/Se ratios are 0.072 (diamictite) and 0.037 (shale), so both ratios have higher mean values in the diamictites (Fig. 2).

Both Te and Se are largely resident in pyrite, as shown by the LA-ICP-MS data (below), so are best assessed normalised to sulphur contents, whereupon diamictites exhibit higher values of both Te/S (mean 0.45) and Se/S (6.12) than shales (Te/S 0.04, Se/S 1.30) (Fig. 2).

Element distribution maps prepared by LA-ICP-MS show that all of the trace elements measured are concentrated in pyrite, and occur at relatively negligible levels in the surrounding matrix (Fig. 3). Analyses of the pyrite show that Se contents are consistently higher in the diamictites (mean 35.1 ± 15.7 ppm) than in the shales (6.3 ± 3.1 ppm) (Fig. 4). There is overlap in the ranges of Te values for diamictites (4.4 ± 5.7 ppm) and shales (0.6 ± 0.5 ppm), but the highest Te values are all recorded in diamictites. The contents of As and Pb show a different distribution (Fig. 4). Arsenic levels are considerably higher in the shales (75.2 ± 79.3 ppm) than in the diamictites (35.2 ± 55.7 ppm), while a wide range of Pb contents are shown by both shales (139.5 ± 194.6 ppm) and diamictites (89.2 ± 123.4 ppm). Gold occurs in diamictite pyrite throughout (Fig. 3). Gold occurs in some shale-hosted pyrite, particularly in outer rims (Parnell *et al.*, 2017), but less widely than in the diamictites. Semi-quantitative analyses of gold in diamictite pyrite yield higher values (mean 0.17 ± 0.30 ppm) than shale pyrite (mean 0.06 ± 0.06 ppm) (Fig. 3).

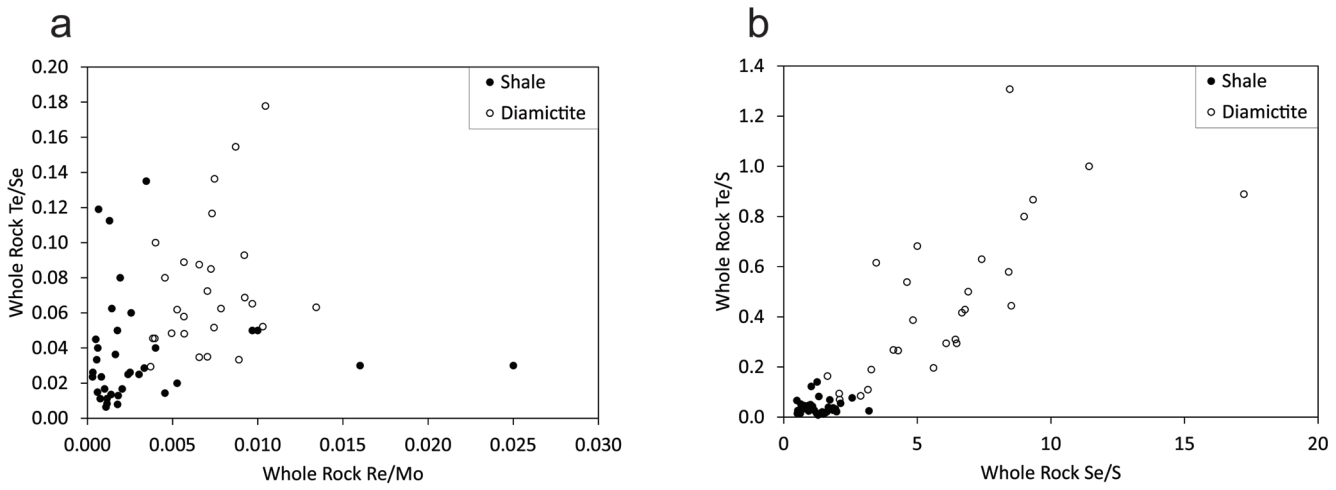

Figure 2 Cross-plots of **(a)** Re/Mo ratio against Te/Se ratio for whole rock samples of diamictites and shales, showing a broad correlation. Both parameters increase with oxygenation of the environment. Samples below detection limit (0.001 ppm) for Re plotted at 50 % of limit. **(b)** Te/S against Se/S for whole rock samples of diamictites and shales.

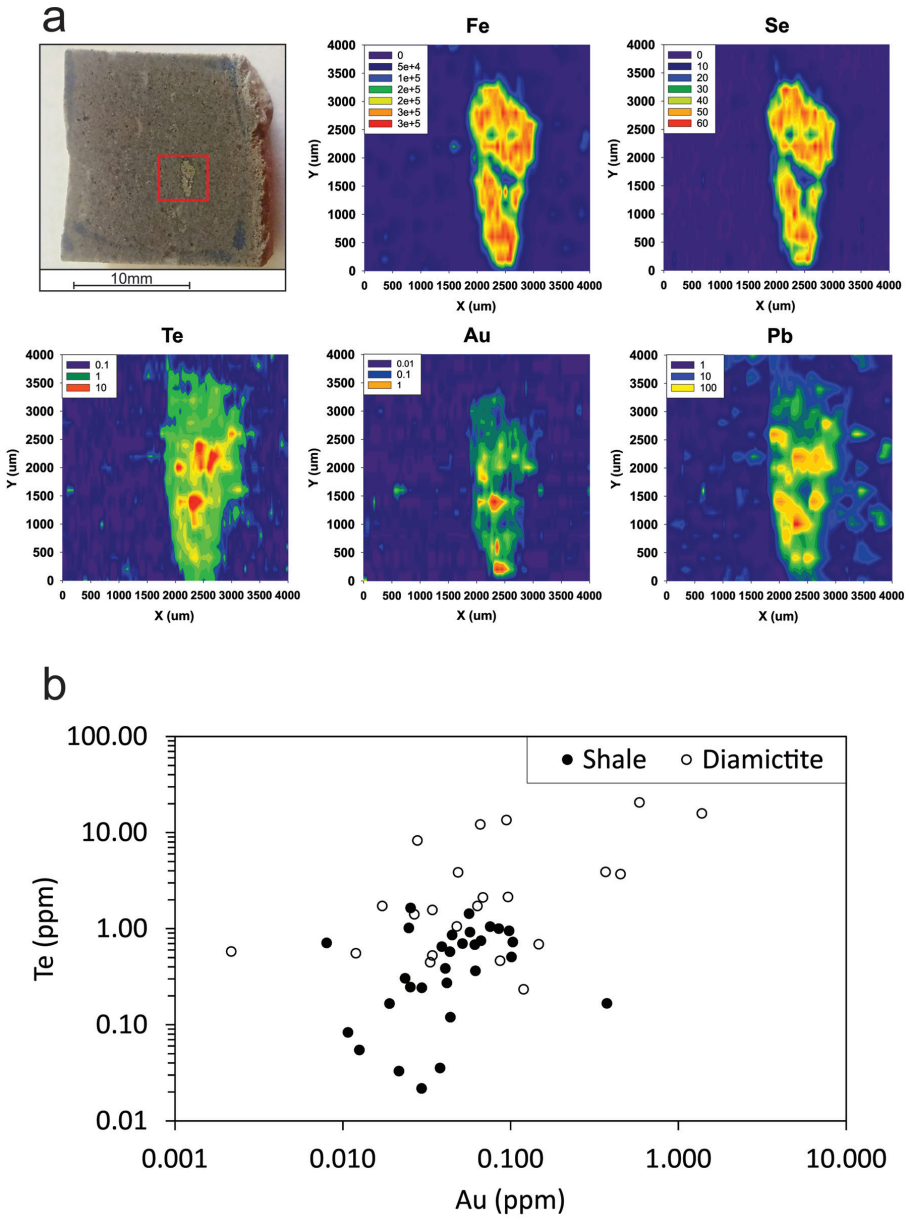

Figure 3 Gold in pyrite, determined by LA-ICP-MS. **(a)** Element maps for pyrite crystal in diamictite, Mull of Oa, Islay, Scotland. Counts in ppm, except Au counts *per* second. **(b)** Cross-plot of Au and Te contents in pyrite. 6 of 7 highest Au values recorded in diamictite.

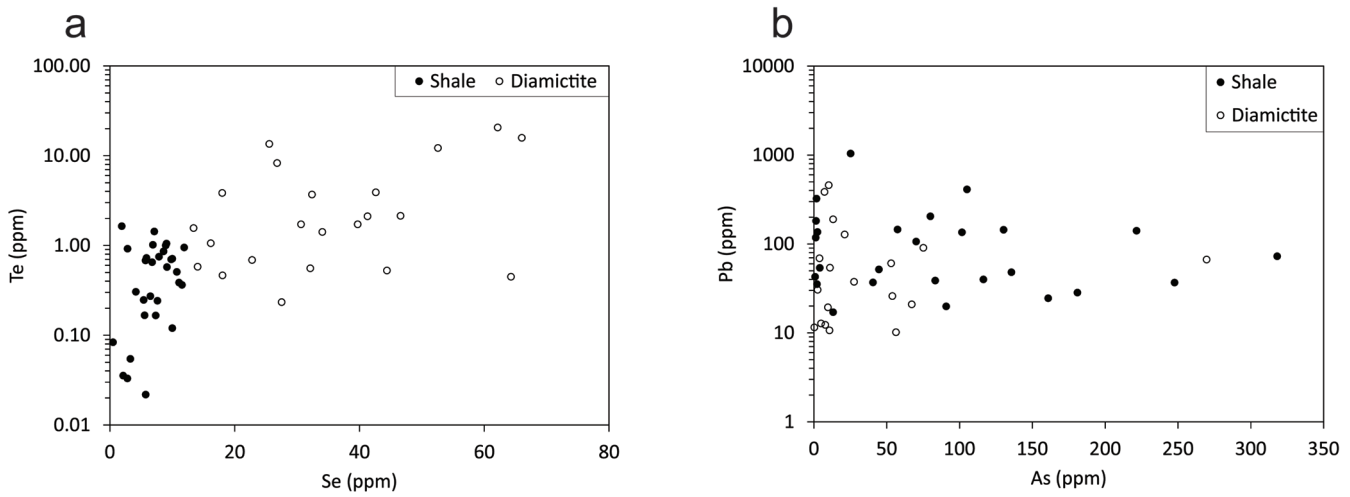

Figure 4 Cross-plots of **(a)** Te against Se contents, and **(b)** As and Pb contents in pyrite, measured by LA-ICP-MS. Highest concentrations of Te are in the diamictites. Arsenic contents are higher in the shales. Lead contents vary highly in both shales and diamictites, due to late addition by hydrothermal fluids.

Discussion

Although pyrite typically forms in reducing environments, microbial sulphate reduction and sulphide precipitation can occur in microniches in otherwise oxidised sediment with Eh up to +300 mV (Jørgensen, 1977). Such microniches are present particularly on particle surfaces, and have been recorded on granite pebbles (Lyew and Sheppard, 1997), which also focus pyrite formation in the diamictites during early diagenesis (Parnell and Boyce, 2017). The texture of pyrite in both facies is clustered micro-crystals (Supplementary Information), so does not control variations in geochemistry.

LA-ICP-MS evidence of trace element residence in pyrite shows that pyrite formation was fundamental to metal enrichment in both diamictites and shales. The LA-ICP-MS data show higher contents of Se, Te and Au in the diamictites. The whole rock and pyrite data bear out the supposition that trace element uptake would have differed in the shales and diamictites, due to contrasting degrees of oxygenation. The diamictites consistently have higher whole rock Re/Mo ratios that signify more oxidising conditions than the shales, which exhibit typical anoxic values (Crusius *et al.,* 1996). The Te/Se ratios are higher in the diamictites, also consistent with more oxidising conditions (Schirmer *et al.,* 2014). A cross-plot of the two ratios shows that the parameters broadly correlate (Fig. 2). The greater degrees of enrichment in Cu, Co, and V in diamictites also points to oxidising conditions, as these elements are typically mobile at high Eh (Fischer and Stewart, 1961). Arsenic shows the opposite trend, of greater contents in the shales, consistent with higher uptake into pyrite in anoxic environments (Berner *et al.,* 2013). Lead is not preferentially concentrated in diamictites or shales, and is variably distributed, particularly in the margins of pyrite crystals (Parnell *et al.,* 2017), which suggests addition from late hydrothermal fluids.

It is argued that the increase in atmospheric oxygenation following the Neoproterozoic glaciations was responsible for increased orogenic gold deposition (Tomkins, 2013). More oxygen would allow higher levels of dissolved gold in seawater (Vlassopoulos and Wood, 1990), which could in turn be incorporated into pyrite precipitated from marine pore waters. This gold is liable to be liberated during metamorphism and deformation, and becomes available to form orogenic gold deposits. Neoproterozoic oxygenation is similarly argued to explain higher selenium contents in mudrocks, selenium contents in pyrite, and a change in selenium isotope fractionation (Large *et al.,* 2014; Stüeken *et al.,* 2015). Tellurium also shows an increase in relative abundance from Precambrian to Phanerozoic due to oxygenation (Schirmer *et al.,* 2014). If the additional oxygen in seawater allows greater uptake of gold and other trace elements in pyrite at/below the sea floor, pyrite in near-surface oxidising environments could have even higher potential to include gold. The evidence, from multiple parameters, of more oxidising conditions in the Dalradian diamictites than in the shales, and a consequent distinctive geochemistry in their pyrite, can explain their relatively high Au contents.

The degree of oxygenation can also influence the uptake of gold in pyrite through the oxidation state of arsenic. Arsenic in pyrite enhances the uptake of a range of trace elements, especially gold (Deditius *et al.,* 2008). In reducing environments, As (I) substitutes for S, while in oxidising conditions As (III) substitutes for Fe (II). Substitution by As (III) leaves vacancies that can accommodate large cations including Au+ (Deditius *et al.,* 2008). Thus pyrite found in more oxidising environments, as in the diamictites, could contain elevated contents of gold, relative to the contents in the shale.

Trace elements in the pyrite are available for further concentration during metamorphism and deformation, including into cross-cutting vein systems (Large *et al.,* 2011). Thus, pyritic sediments may be a protolith for orogenic gold deposits (*e.g.,* Pitcairn, 2011; Tomkins, 2013). Apart from evidence of Pb-rich fluid at the outermost rim of pyrite in some shale samples, the Dalradian pyrite chemistry is relatively uniform, showing that it has not been overprinted by metamorphism. The data reported here suggest that this model may be applicable to orogenic gold deposits in the Dalradian Supergroup, which are mined in both Scotland and Ireland (Fig. 1). However, the data imply that the diamictite-bearing section, which at the type locality of the Port Askaig Formation is 700 m thick, could contribute significantly to the protolith, which otherwise would be assumed to consist only of shales. The gold content in several diamictite pyrites (Fig. 3) exceeds the 0.25 ppm threshold suggested as indicative of gold ore potential (Large *et al.* 2011). The diamictites sampled occur over 450 km, representing a large volume of rock with elevated trace element contents. The pyrite in Dalradian diamictites exemplifies a global occurrence of pyrite in 'Snowball Earth' diamictites (Parnell and Boyce, 2017), whose metallogenic potential deserves to be investigated.

Conclusions

Data sets for trace elements in both whole rocks and pyrite show a contrast between diamictites and shales in the Argyll subgroup. In particular:

(i) Trace elements, including Se, Te, As, Pb and Au, were sequestered especially into pyrite.

(ii) Tellurium and Se, and also redox-sensitive elements Cu, Co, and V, uptake was higher into the diamictites than into the shales.

(iii) Gold enrichment also occurs in the pyrite, especially in diamictite-hosted pyrite.

(iv) Multiple parameters indicate a greater degree of oxygenation in the diamictites.

Combined, these observations suggest that greater oxygenation engendered greater uptake of trace elements, including Te, Se and Au into pyrite. The model of an anoxic shale protolith for orogenic gold deposits pertains because most pyrite forms in anoxic sediments. However, an awareness of the potential trace element reservoir in more oxygenated environments may lead to the discovery of hitherto unknown gold prospects.

Acknowledgements

This work was supported by the NERC under Grant number NE/L001764/1. AJB is funded by NERC support of the Isotope Community Support Facility at SUERC. We are grateful to S. Mojzsis and I. Mukherjee for critical reviews, and A. Spencer and K. Mackay for help with sampling.

Editor: Eric Oelkers

Additional Information

Supplementary Information accompanies this letter at http://www.geochemicalperspectivesletters.org/article1812.

Cite this letter as: Parnell, J., Perez, M., Armstrong, J., Bullock, L., Feldmann, J., Boyce, A.J. (2018) Geochemistry and metallogeny of Neoproterozoic pyrite in oxic and anoxic sediments. *Geochem. Persp. Let.* 7, 12–16.

References

Berner, Z.A., Puchelt, H., Nöltner, T., Kramar, U. (2013) Pyrite geochemistry in the Toarcian Posidonia Shale of south-west Germany: Evidence for contrasting trace-element patterns of diagenetic and syngenetic pyrites. *Sedimentology* 60, 548-573.

Crusius, J., Calvert, S., Pedersen, T., Sage, D. (1996) Rhenium and molybdenum enrichments in sediments as indicators of oxic, suboxic and sulfidic conditions of deposition. *Earth and Planetary Science Letters* 145, 65-78.

Deditius, A.P., Utsunomiya, S., Renock, D., Ewing, R.C., Ramana, C.V., Becker, U., Kesler, S.E. (2008) A proposed new type of arsenian pyrite: Composition, nanostructure and geological significance. *Geochimica et Cosmochimica Acta* 72, 2919-2933.

Fischer, R.P., Stewart, J.H. (1961) Copper, vanadium and uranium deposits in sandstone. Their distribution and geochemical cycles. *Economic Geology* 56, 509-520.

Gaboury, D. (2013) Does gold in orogenic deposits come from pyrite in deeply buried carbon-rich sediments?: Insight from volatiles in fluid inclusions. *Geology* 41, 1207-1210.

Jørgensen, B.B. (1977) Bacterial sulfate reduction within reduced microniches of oxidized marine sediments. *Marine Biology* 41, 7-17.

Large, R.R., Bull, S.W., Maslennikov, V.V. (2011) A carbonaceous sedimentary source-rock model for Carlin-type and orogenic gold deposits. *Economic Geology* 106, 331-358.

Large, R.R., Hapin, J.A., Danyushevsky, L.V., Maslennikov, V.V., Bull, S.W., Long, J.A., Gregory, D.D., Lounejeva, E., Lyons, T.W., Sack, P.J., McGoldrick, P.J., Calver, C.R. (2014) Trace element content of sedimentary pyrite as a new proxy for deep-time ocean-atmosphere evolution. *Earth and Planetary Science Letters* 389, 209-220.

Lyew, D., Sheppard, J.D. (1997) Effects of physical parameters of a gravel bed on the activity of sulphate-reducing bacteria in the presence of acid mine drainage. *Journal of Chemical Technology and Biotechnology* 70, 223-230.

Parnell, J., Boyce, A.J. (2017) Microbial sulphate reduction during Neoproterozoic glaciation, Port Askaig Formation, UK. *Journal of the Geological Society, London* 174, 850-854.

Parnell, J., Perez, M., Armstrong, J., Bullock, L., Feldmann, J., Boyce, A.J. (2017) A black shale protolith for gold-tellurium mineralization in the Dalradian Supergroup (Neoproterozoic) of Britain and Ireland. *Applied Earth Science* 126, 161-175, doi: 10.1080/03717453.2017.1404682.

Pitcairn, I.K. (2011) Background concentrations of gold in different rock types. *Applied Earth Science* 120, 31-38.

Prave, A.R., Fallick, A.E., Thomas, C.W., Graham, C.M. (2009) A composite C-isotope profile for the Neoproterozoic Dalradian Supergroup of Scotland. *Journal of the Geological Society, London* 166, 845-857.

Schirmer, T., Koschinsky, A., Bau, M. (2014) The ratio of tellurium and selenium in geological material as a possible paleo-redox proxy. *Chemical Geology* 376, 44-51.

Stüeken, E.E., Buick, R., Bekker, A., Catling, D., Foriel, J., Guy, B.M., Kah, L.C., Machel, H.G., Montañez, I.P., Poulton, S.W. (2015) The evolution of the global selenium cycle: Secular trends in Se isotopes and abundances. *Geochimica et Cosmochimica Acta* 162, 109-125.

Tabelin, C.B., Igarashi, T., Tamoto, S., Takahashi, R. (2012) The roles of pyrite and calcite in the mobilization of arsenic and lead from hydrothermally altered rocks excavated in Hokkaido, Japan. *Journal of Geochemical Exploration* 119, 17-31.

Tomkins, A.G. (2013) A biogeochemical influence on the secular distribution of orogenic gold. *Economic Geology* 108, 193-197.

Vlassopoulos, D., Wood, S.A. (1990) Gold speciation in natural waters: Solubility and hydrolysis reactions of gold in aqueous solution. *Geochimica et Cosmochimica Acta* 54, 3-12.